

Effect of a Block Copolymer on the Kinetics of Spinodal Decomposition of Polymer Blends. 2. Scaled Structure Factor

Tatsuo Izumitani[†] and Takeji Hashimoto*

Department of Polymer Chemistry, Kyoto University, Kyoto 606, Japan

Received August 30, 1993; Revised Manuscript Received January 3, 1994*

ABSTRACT: Effects of adding a small amount of a block copolymer to polymer blends composed of the same constituent polymers as the block copolymer on the kinetics of later-stage spinodal decomposition (SD) were investigated by a time-resolved light scattering at three different temperatures in a deep quench condition. Changes in the scaled structure factors $F(x) = q_m(t;T,\phi)^3 I(x,t;T,\phi)$ with $x = q/q_m(t;T,\phi)$ as a function of the composition of the block copolymer ϕ were analyzed at various temperatures T , where $q_m(t;T,\phi)$ is the magnitude of the scattering vector q at which the first-order peak of the scattering intensity profile $I(q,t;T,\phi)$ appears. It was found that the scaled structure factor obtained for each blend was almost identical, independent of the amount of the block copolymer. The time evolution of the global or the local structure is slowed with increasing block copolymer content. However, the dynamical self-similarity is held during the SD and the self-similar structure evolved is independent of ϕ , the amount of the block copolymer added to the blends, at least within the time range of our experiments and $\phi \leq 0.06$.

I. Introduction

In our previous paper,¹ we investigated the effect of adding a small amount of a block copolymer to the polymer blends composed of the same constituent polymers as the block copolymer on the kinetics of early-to-late stage spinodal decomposition (SD). We analyzed the time changes of the magnitude of the scattering vector $q_m(t;T,\phi)$ and the peak of the scattering intensity $I_m(t;T,\phi)$, where t is time, T is the phase separation temperature, and ϕ is the amount of the block copolymer. The system studied was poly(styrene-*ran*-butadiene) (SBR)/polybutadiene (PB)/SBR-*block*-polybutadiene. Here SBR-*block*-polybutadiene is a diblock copolymer composed of the SBR block chain and the polybutadiene block chain. We designate it as SBR-*b*-PB. In the early stage of SD, the time evolution of the concentration fluctuations is well approximated by linearized theory.^{2,3} In the late stage of SD,^{4,5} we found the validity of the scaling postulate proposed by Langer et al.⁶ for each blend; i.e., the time changes of q_m and I_m at different temperatures fall onto respective master curves on the reduced plots: reduced intensity $\tilde{I}_m(\tau)$ and reduced scattering vector $Q_m(\tau)$ plotted against reduced time τ . Here the reduced quantities are defined as follows:

$$\tau \equiv t/t_c(T), \quad t_c(T) = q_m^{-2}(0;T) D_{app}^{-1}(T) \quad (1)$$

$$Q_m(\tau) \equiv q_m(t;T)/q_m(0;T) \quad (2)$$

$$\tilde{I}_m(\tau) \equiv I_m(t,T) q_m^3(0;T) / \int_{q'}^{q''} q^2 I(q,t;T) dq \quad (3)$$

$t_c(T)$ is the characteristic time of the blend at temperature T , $q_m(0;T)$ is the characteristic wavenumber of the blend at T , i.e., the wavenumber of the Fourier mode of the concentration fluctuations which grows at the maximum rate in the early stage, and $D_{app}(T)$ is the collective diffusion coefficient of the blend at T . $q_m(t,T)$ is the wavenumber of the Fourier mode which has the highest intensity at t and T , i.e., the magnitude of the scattering vector $q = (4\pi/\lambda) \sin(\theta/2)$ (λ and θ being the wavelength and the

scattering angle in the medium, respectively) for the maximum scattering intensity $I_m(t;T)$ and q' and q'' are respectively the magnitude of the scattering vectors below and above which the integrand goes effectively zero. $I(q,t;T)$ is the scattering intensity distribution from the blend at t and T . However, the master curves of $\tilde{I}_m(\tau)$ and $Q_m(\tau)$ obtained for each blend were found¹ to depend on ϕ , thus showing a "branch (or nonuniversality)" in the reduced plots. The branching designated "B-branching" where B stands for block copolymer is attributed to a reduction of interfacial tension as a consequence of localization of the block copolymers at interfaces between the phase-separating domains during the ordering process. The nonuniversal nature of the coarsening behavior with ϕ , as observed with $Q_m(\tau)$ and $\tilde{I}_m(\tau)$, indicates that the block copolymer affects not only the time and spatial scales of the ordering process but also the mechanism of the ordering process. As concentration fluctuations grow and the interface between the two domains is formed, the copolymer chains tend to diffuse into the interfaces and to localize there. The localized copolymer then reduces the interfacial tension, which in turn affects the coarsening due to the hydrodynamic effects,^{7,8} and the interface dynamics.⁹ In the coarsening process, the interfacial area is reduced, which increases the number density of the copolymer at the interface. The interface may be eventually saturated with the copolymer molecules, and further coarsening may be hindered, leading to the pinning of the domain growth.

In this paper, we investigate further the scaled structure factor $F(x,t;T,\phi)$ as a function of volume fraction ϕ (ϕ is nearly equal to the weight fraction for our case) and T , where $F(x,t;T,\phi)$ is defined by¹⁰

$$F(x,t;T,\phi) \equiv q_m(t;T,\phi)^3 I(x,t;T,\phi) \quad (4)$$

with

$$x \equiv q/q_m(t;T,\phi) \quad (5)$$

It may be in order to briefly review earlier work on the scaled structure for pure blends without the copolymer, before going into detailed discussion on the effect of the copolymer on the scaled structure factor.

The time evolutions of $q_m(t;T)$ and $I_m(t;T)$ have been traditionally characterized by such scaling laws as¹¹

[†] Present address: Daicel Chemical Ind., Ltd., 1239 Shinzaike, Aboshi-ku, Himeji, Hyogo 671-12, Japan.

* Abstract published in *Advance ACS Abstracts*, February 15, 1994.

$$q_m(t;T) \sim t^{-\alpha} \quad (6)$$

and

$$I_m(t;T) \sim t^{\beta} \quad (7)$$

The scaling exponents α and β in the intermediate stage have been found to show the relationship of

$$\beta > 3\alpha \quad (8)$$

This relation changes into

$$\beta = 3\alpha \quad (9)$$

in the late stage SD. The crossover of the behavior from eq 8 to eq 9 has been used to find the crossover between the intermediate and the late stages. For pure blends without the block copolymers, the scaled structure factor $F(x,t;T)$ was found to increase and sharpen with time t in the intermediate stage.^{12,13} However, in the late stage, $F(x,t;T)$ at $x \lesssim 2$ reaches a time-independent universal scaling function $S(x;T)$,¹² supporting the dynamical scaling hypothesis¹⁰ for the time evolution of the global structure, in that the growth of the global structure occurs with dynamical self-similarity.

In our previous results,¹²⁻¹⁵ the $F(x,t;T)$ at large x (>2) is not universal but rather increasing with t in the early time of the late stage, implying that the local structure such as interface structure cannot be scaled with the length parameter $1/q_m(t;T)$ characterizing the global structure. Namely, relevant parameters such as $\Sigma(t;T)$ and $t_1(t;T)$ characterizing the time evolution of the local structure change with t with the following scaling laws which are different from that for the global parameter given by eq 6,

$$\Sigma(t;T) \sim t^{-\gamma} \quad (10)$$

and

$$t_1(t;T) \sim t^{-\delta} \quad (11)$$

where Σ and t_1 are the interfacial area density (interface area per unit volume) and the characteristic interface thickness,¹⁴ respectively. Our previous analysis¹⁵ elucidated that

$$\gamma > \alpha \quad (12)$$

in the late stage I but that

$$\gamma = \alpha \quad (13)$$

in the late stage II. The relation given by eq 12 and the nonnegligible contribution of the interface thickness to $F(x,t;T)$ at larger x were found¹⁴ to give nonuniversality of $F(x,t;T)$ at large x .

In this study, we aimed to extend our previous study of the effect of the block copolymer on the time evolution of the global structure to that on the time evolution of the local structure. We aimed to study also the time change of the scaled structure in order to further characterize the shape of the growing structure for the SBR/PB/SBR-*b*-PB mixtures.

II. Experimental Methods

The specimens used in these studies were poly(styrene-*ran*-butadiene) (SBR), polybutadiene (PB), and SBR-*b*-PB. SBR and PB were coded as SBR1 and PB2, respectively. The

Table 1. Characteristics of Polymers Used in This Work

specimen code	$\bar{M}_n \times 10^{-4}$	\bar{M}_w/\bar{M}_n	content (%)		microstructure (%) ^f		
			w_{PS}^d	w_{SBR}^e	vinyl	cis-1,4	trans-1,4
SBR1 ^a	10.0	1.18	20	100	61	16	23
PB2 ^b	16.5	1.16	0	0	46	19	35
SBR- <i>b</i> -PB ^c	21.1		30	50	51	20	29

^a Poly(styrene-*ran*-butadiene). ^b Poly(butadiene). ^c Poly[(styrene-*ran*-butadiene)-*block*-butadiene], i.e., poly(SBR-*block*-butadiene). ^d Weight percentage of styrene in poly(styrene-*ran*-butadiene). ^e Weight percentage of poly(styrene-*ran*-butadiene) in a given polymer or block copolymer. ^f Microstructure in the butadiene unit in each polymer.

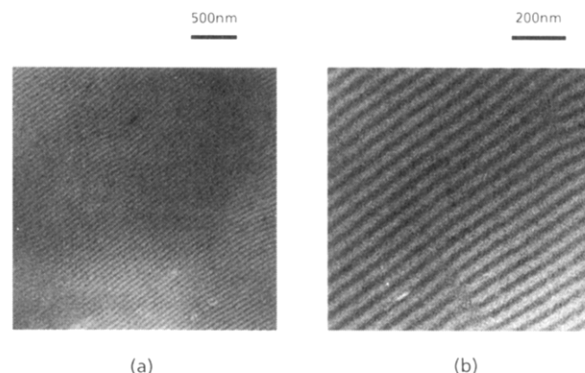


Figure 1. Transmission electron micrographs of an ultrathin section of neat SBR-*b*-PB. The section was stained with osmium tetroxide. a and b represent the lower and higher magnifications, respectively.

characteristics of the specimens are listed in Table 1. Three kinds of blends, coded B0, B3, and B6 having the compositions SBR/PB/SBR-*b*-PB = 58.0/42.0/0, 56.3/40.7/3.0, and 54.5/39.5/6.0 (wt %/wt %/wt %), respectively, were cast into thin films about 0.2 mm thick using toluene as a neutral solvent. The films were further dried in a vacuum oven at room temperature until their weight became constant. The as-cast films have phase-separated structures via SD during the solvent evaporation process. They could not be made single phase by temperature elevation without thermal degradation. Thus we prepared single-phase blends by a homogenization process involving a Baker's transformation as described elsewhere.¹⁶ The homogenized film specimen was sandwiched between thin glass plates in a sample holder, and then the film specimen was subjected to a temperature jump (T -jump) to a given phase separation temperature T . The dynamics of the unmixing process was observed *in situ* by the time-resolved light scattering method described elsewhere.¹⁷ The time right after the homogenization was taken as the origin of time t . Turbidity and solid angle corrections were applied to the observed intensity $I(q,t;T,\phi)$.¹⁵ The phase-separation conditions were estimated by the parameter ϵ_T , characterizing the quench depth from the relation

$$\epsilon_T = (\chi_{\text{eff}}(T) - \chi_s)/\chi_s \quad (14)$$

where $\chi_{\text{eff}}(T)$ is the effective Flory interaction parameter (χ -parameter) per segment between PB and SBR and χ_s is the value $\chi_{\text{eff}}(T)$ at the spinodal temperature. The values of ϵ_T for all mixtures prepared were larger than unity, corresponding to deep quench conditions, as in our previous paper.¹

The SBR-*b*-PB was stained with osmium tetroxide vapor and was then subjected to ultramicrotoming into an ultrathin section using a Reichert-Nissei Ultracut N with a cryogenic FC 4E. The transmission electron microscopic (TEM) investigation was carried out with a Nihon Denshi JEM 1200EX II transmission electron microscope operated at 100 kV.

III. Experimental Results

Figure 1 shows electron micrographs of an ultrathin section of neat SBR-*b*-PB. The dark regions correspond to polybutadiene (PB) microdomains selectively stained

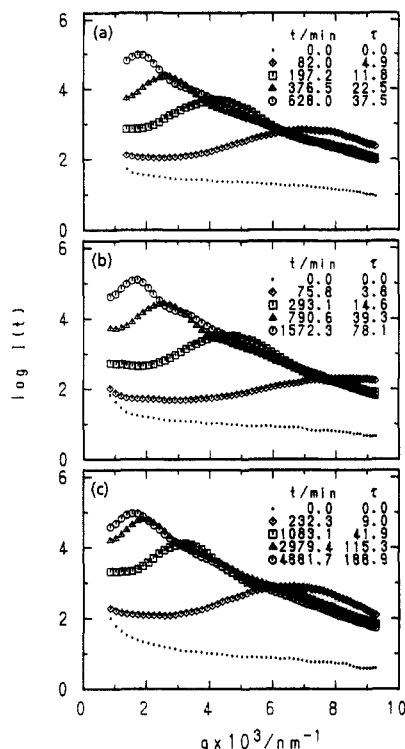


Figure 2. Time evolution of light scattering profiles for (a) B0, (b) B3, and (c) B6 during the spinodal decomposition at 50 °C. t and τ refer to the real and reduced times after onset of spinodal decomposition.

with osmium tetroxide, and the bright regions correspond to relatively less stained SBR microdomains. The micrograph suggests the microdomain structure of lamellar morphology composed of the lamellae rich in SBR and those rich in PB. The content of styrene and the molecular weight of SBR in the SBR-*b*-PB are almost the same as those of SBR1. Furthermore, the microstructure and the molecular weight of PB in the SBR-*b*-PB are almost the same as those of homopolybutadiene PB2. The χ -value at the spinodal point of the binary polymer mixture SBR1/PB2 50/50 (v/v) ($\chi_{s,macro}$) is smaller than that of the block copolymer SBR-*b*-PB ($\chi_{s,micro}$). Therefore, liquid-liquid macrophase separation of the polymeric mixture occurs prior to the microphase separation of the corresponding block copolymer.¹⁸

Parts a-c of Figure 2 show the time evolution of light scattering profiles during SD at 50 °C for the blends B0, B3, and B6, respectively. With increasing time after phase separation, the scattering maximum appears at the large q limit covered in our experiment, and this maximum shifts toward smaller q and the peak intensity increases, indicating the coarsening of the structure self-assembled via SD. Close observation of the results clearly indicates that the coarsening process is slowed on addition of the block copolymer.

The time changes of the peak scattering vector $q_m(t;T,\phi)$ are shown in Figure 3. In these figures, parts a-c represent the effects of block copolymer composition on the coarsening process at 50, 60, and 70 °C, respectively. At each temperature, the coarsening rate decreases with an increasing amount of the block copolymer, i.e., the more the block copolymer content, the longer the time required to reach given levels of $q_m(t;T,\phi)$.

IV. Scaled Structure Factor

If the time evolution of the pattern at a given T obeys the dynamical scaling law,¹⁰ the scattering function $I(q,t;T)$ is given in terms of the universal scaling function $S(x)$

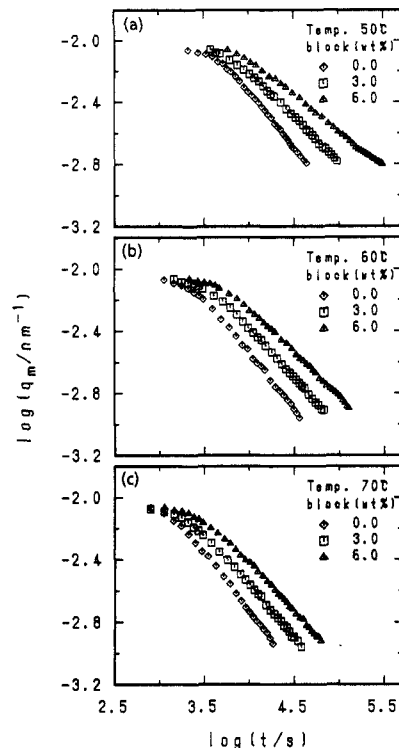


Figure 3. Time change of the characteristic wavenumber $q_m(t)$ for blends with various block copolymer compositions at (a) 50, (b) 60, and (c) 70 °C.

$$I(q,t;T) \sim \langle \eta(t;T)^2 \rangle q_m(t;T)^{-3} S(x) \quad (15)$$

where $\langle \eta(t;T)^2 \rangle$ is the mean-squared fluctuation of the refractive index relevant to the pattern at t and T . Thus, from eqs 4 and 15, the scaled structure factor $F(x,T)$ is related to $S(x)$ by

$$F(x,t) \sim \langle \eta(t;T)^2 \rangle S(x) \quad (16)$$

In the late stage in which $\langle \eta(t;T)^2 \rangle$ becomes the equilibrium value $\langle \eta(T)^2 \rangle_e$ determined by the phase diagram and T ,

$$\langle \eta(t;T)^2 \rangle = \langle \eta(T)^2 \rangle_e \quad (17)$$

Thus, in this case, $F(x;T)$ at a given T becomes universal with t . Furthermore, the reduced $\bar{F}(x,t)$ defined by

$$\bar{F}(x,t) \equiv F(x,t;T) / \int_{q'}^{q''} q^2 I(q,t;T) dq \sim F(x,t;T) / \langle \eta(T)^2 \rangle_e \quad (18)$$

becomes universal with T also, i.e.,

$$\bar{F}(x,t) \sim S(x) \quad (19)$$

Here q' and q'' are respectively the magnitudes of the scattering vectors below and above which the integrand goes effectively zero. In our analysis,¹ $\langle \eta(T,\phi)^2 \rangle_e$ was assumed to be constant independent of temperature, since the temperature range covered is very narrow and far from the critical point; i.e., ϵ_T is almost independent T .

Figures 4 and 5 show the scaled structure factor $F(x,t;T,\phi)$ at 50 °C plotted as a function of x for the blends of B0 and B6, respectively. The later stage SD for the blends with or without the block copolymer is seen to be divided into the two stages: the intermediate and late stages, as in the previous result.^{13,19} In the intermediate stage (Figures 4a and 5a), the mean-squared fluctuation $\langle \eta(t;T,\phi)^2 \rangle$ of the refractive index between the two phases does not yet reach an equilibrium value $\langle \eta(T;\phi)^2 \rangle_e$ but

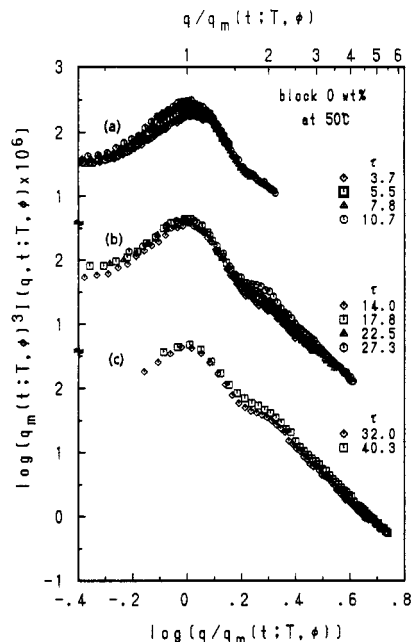


Figure 4. Scaled structure factor $F(x, t; T, \phi)$ in the intermediate stage (a) and the late stage (b and c) for B0 at 50 °C.

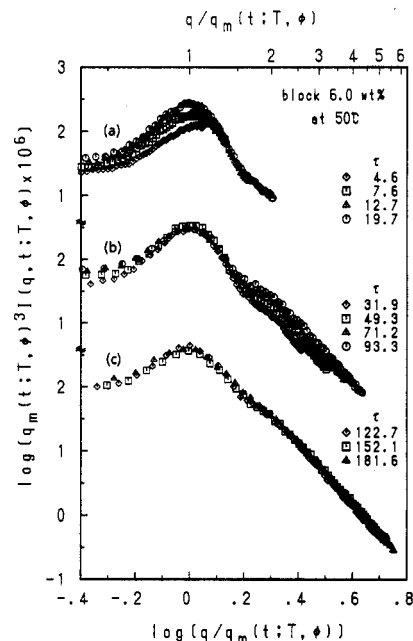


Figure 5. Scaled structure factor $F(x, t; T, \phi)$ in the intermediate stage (a) and the late stage (b and c) for B6 at 50 °C.

increases with time t . Hence, $F(x, t; T, \phi)$ for different times do not superimpose but increase with time. This feature is independent of the amount of the copolymer added to the mixture. In the late stage (Figures 4b, 4c, 5b, and 5c), however, $\langle \eta(t; T, \phi)^2 \rangle$ reaches the equilibrium value $\langle \eta(T; \phi)^2 \rangle$, independent of time, and hence $F(x, t; T, \phi)$ at $x < 2$ becomes independent of time. In this stage the growth of the global domain structure satisfies the dynamical scaling hypothesis¹⁰ and is scaled with the single length parameter $1/q_m(t; T, \phi)$. However, the scaled structure factors are not universal with t at higher reduced wave-number $x > 2$, indicating that the local structure cannot be scaled with the length parameter $1/q_m(t; T, \phi)$. The growth of the local structure should obey a dynamical scaling law different from that of the global length parameter, as will be discussed in section V.

Parts a and b of Figure 6 show the time changes of the intensity of the scaled structure factor $F(x, t; T, \phi)$ at $x =$

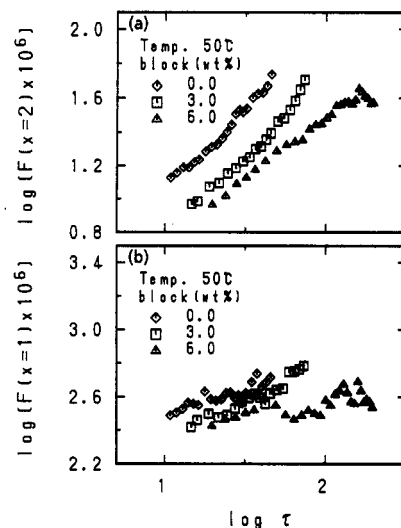


Figure 6. Intensity change of the scaled structure factor $F(x, t; T, \phi)$ with the reduced time τ at (a) $x = 2$ and (b) $x = 1$ for blends with various block copolymer compositions at 50 °C.

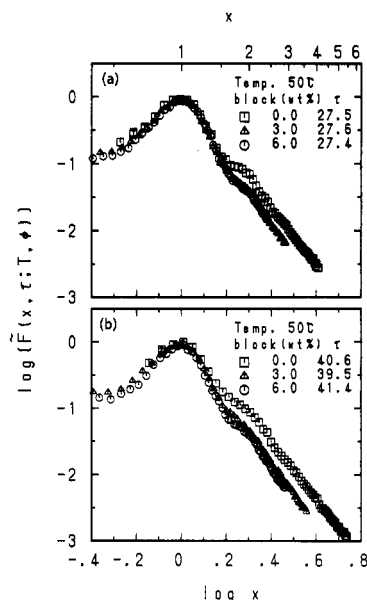


Figure 7. Reduced scaled structure factor $\tilde{F}(x, t; T, \phi)$ at the same reduced time (a) $\tau \approx 27$ and (b) $\tau \approx 40$ for the blends with various block copolymer compositions at 50 °C.

2 and 1 for blends with various block copolymer contents, respectively. The intensity of the scaled structure factor at $x = 1$ (part b) reaches an almost constant level in the late stage but that at $x = 2$ still increases with time, indicating the local structure still changes with time t in the late stage or the local structure cannot be scaled with the length parameter $1/q_m(t; T, \phi)$ relevant to the global structure. The higher the amount of the copolymer ϕ , the slower is the time evolution of the local structure even in the reduced time scale.

Figure 7 shows effects of the block copolymer on the reduced scaled structure factor $\tilde{F}(x, \tau; T, \phi) \equiv F(x, \tau; T, \phi)/F(x=1, \tau; T, \phi)$ at 50 °C. Here, we compare $\tilde{F}(x, \tau; T, \phi)$ for the blends with the various block copolymer contents at nearly the same reduced time, $\tau = 27$ (Figure 7a) and $\tau = 40$ (Figure 7b). At the same reduced time, the $\tilde{F}(x, \tau; T, \phi)$'s at $x < 2$ are almost universal with ϕ , indicating that the global structure is almost independent of ϕ and is not affected by the amount of the copolymer added. However, the intensity of $\tilde{F}(x, \tau; T, \phi)$ at $x > 2$ tends to decrease with ϕ , indicating that the local structure depends on ϕ , the greater the amount of the block copolymer, the

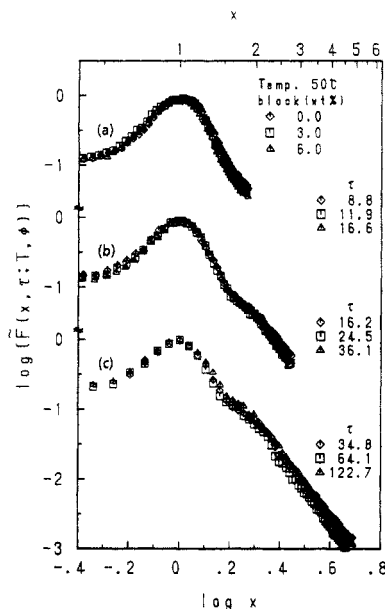


Figure 8. Reduced scaled structure factor $\tilde{F}(x, t; T, \phi)$ for blends with various block copolymer compositions at the same peak scattering vector $q_m(t; T, \phi)$: (a) 5.0×10^{-3} , (b) 3.3×10^{-3} , and (c) $1.9 \times 10^{-3} \text{ nm}^{-1}$ at 50°C .

less developed the structure is. The intensity of F at $x > 2$ for the blend with a given copolymer content ϕ is expected to reach that for the blend with $\phi = 0$ at a much later time even in the reduced time scale, as is shown in Figure 6a and will be shown in Figure 8. This phenomenon is closely related to the B-branch effect.¹

Figure 8 shows a comparison of $\tilde{F}(x, \tau; T, \phi)$ obtained for the blends with various block copolymer contents at the same global size; i.e., at the same peak scattering vector $q_m(t; T, \phi) = 5.0 \times 10^{-3}$ (a), 3.3×10^{-3} (b), and $1.9 \times 10^{-3} \text{ nm}^{-1}$ (c). It was found that the scaled structure factor obtained for each blend was almost identical, independent of the amount of the block copolymer. The time evolution of the global or the local structure is slowed with increasing block copolymer content. However, the structure evolved at the time renormalized with respect to this slowing effect is independent of whether the block copolymer exists in the blends or not, at least within the time range of our experiments.

V. Interface Structure

We analyzed the time evolution of the interface structure according to the method described previously.^{14,15} The reduced scattered intensity defined as

$$\tilde{I}(q, t; T, \phi) = I(q, t; T, \phi) / \int_{q'} q'^2 I(q', t; T, \phi) dq' \quad (20)$$

is given, in the Porod's law^{20,21} regime, by

$$\tilde{I}(q, t; T, \phi) = [\pi f(1-f)]^{-1} \Sigma(t; T, \phi) q^{-4} \exp[-\sigma(t; T, \phi)^2 q^2] \quad (21)$$

where $\sigma(t; T, \phi)$ is the parameter related to the characteristic interface thickness $t_I(t; \phi)$ by²²

$$t_I = (2\pi)^{1/2} \sigma(t; T, \phi) \quad (22)$$

and f is volume fraction of one of the domains.

Figure 9 shows the time change of $\ln[q^4 \tilde{I}(q, t; T, \phi)]$ vs q^2 for B0 (a), B3 (b), and B6 (c) at 50°C . The plots show a good linear relation over a wide range of q in the late

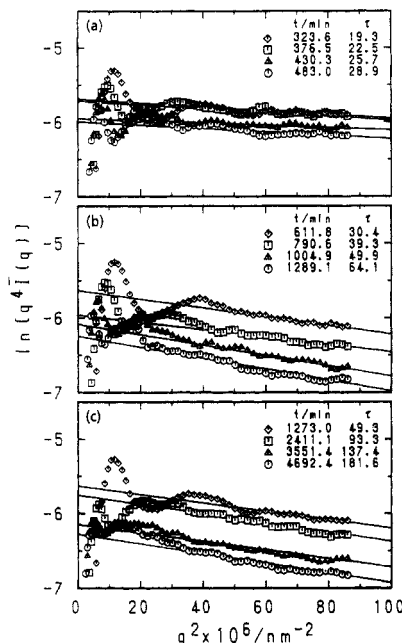


Figure 9. Plots of $\ln[q^4 \tilde{I}(q, t; T, \phi)]$ versus q^2 at different times t or τ for (a) B0, (b) B3, and (c) B6 at 50°C .

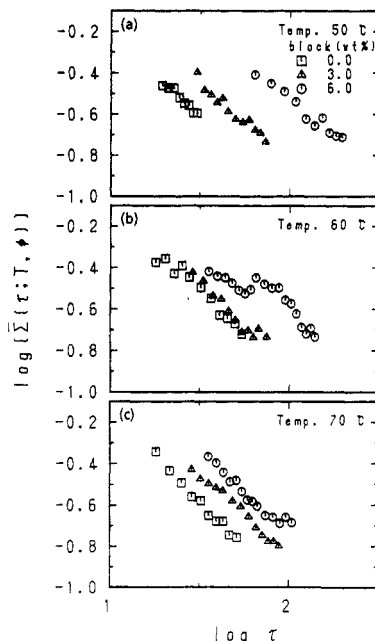


Figure 10. Reduced interfacial area density $\tilde{\Sigma}(t; T, \phi)$ plotted as a function of reduced time τ for blends with various block copolymer compositions at (a) 50, (b) 60, and (c) 70°C .

stage of SD. The plots yielded $\sigma(t; T, \phi)$ and $\Sigma(t; T, \phi)$ from the slopes and the intercepts at $q = 0$, respectively.

$\Sigma(t; T, \phi)$ has a dimension of wavenumbers, and hence we designate it as the "local wavenumber" in contrast to the $q_m(t; T, \phi)$ characterizing the "global wavenumber". We attempt to scale $\Sigma(t; T, \phi)$ with the characteristic wavenumber $q_m(0; T, \phi)$. We defined the dimensionless quantities by¹⁵

$$\tilde{\Sigma}(t; T, \phi) = \Sigma(t; T, \phi) / q_m(0; T, \phi) \quad (23)$$

In order to check the possibility of extending the scaling postulate by Langer et al. on the global structure to the local structure, $\tilde{\Sigma}(t; T, \phi)$ is plotted double-logarithmically as a function of τ .

Figure 10 shows double-logarithmic plots of $\tilde{\Sigma}(t; T, \phi)$ as a function of τ for blends with various copolymer compositions at 50 (a), 60 (b), and 70°C (c). It is clearly

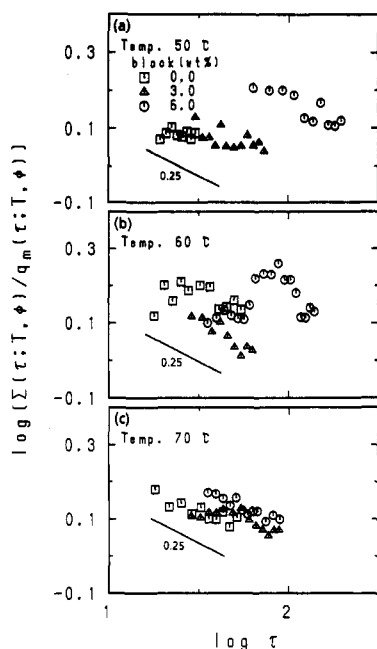


Figure 11. $\Sigma(\tau; T, \phi)/q_m(\tau; T, \phi)$ plotted as a function of τ on a double-logarithmic scale for blends with various block copolymer compositions at (a) 50, (b) 60, and (c) 70 °C.

shown that $\bar{\Sigma}(\tau; T, \phi)$ obeys the scaling law given by

$$\bar{\Sigma}(\tau; T, \phi) \sim \tau^{-\gamma} \quad (24)$$

with a prefactor which explicitly depends on ϕ .

In our previous paper,¹⁵ we reported that the scaling postulate can be extended to the local structure for the mixtures without the copolymer; i.e., the time evolution of the interfacial area density becomes universal with T when Σ is reduced with the T -dependent characteristic wavenumber $q_m(0; T)$ and t is reduced with the T -dependent characteristic time $t_c(T)$. However, in the case of the blends with the copolymer, the plot of $\bar{\Sigma}(\tau; T, \phi)$ versus τ is roughly universal with T , as in the case of the blends without the copolymer, but is not definitely universal with ϕ . The more the block copolymer content, the longer the reduced time to reach the same level of $\bar{\Sigma}(\tau; T, \phi)$. This fact suggests that the block copolymer slows down the evolution of the local structure, too.

The time evolution of the local wavenumber $\Sigma(t; T, \phi)$ in the late stage was compared with that of global wavenumber $q_m(t; T, \phi)$. The results are shown in Figure 12, where the change of $\Sigma(\tau; T, \phi)/q_m(\tau; T, \phi) (\sim \tau^{-(\gamma-\alpha)})$ is plotted against the reduced time τ on a double-logarithmic scale for various block copolymer compositions at 50 (a), 60 (b), and 70 °C (c). In a previous paper,¹⁵ we reported that $\gamma > \alpha$ in an earlier time of the late stage (the late stage I), but $\gamma = \alpha$ in a later time of the late stage (the late stage II) and the reduced plot tends to show such a tendency that

$$\gamma - \alpha \simeq 0.25, \text{ at } \tau < \tau_{cr,2} = 120 \quad (25)$$

for the late stage I ($\tau_{cr,2}$ being the crossover reduced time between the late stage I and the late stage II) and

$$\gamma - \alpha = 0, \text{ at } \tau > \tau_{cr,2} \quad (26)$$

for the late stage II. In our case, we found a trend similar to that given by eq 25, i.e., the trend typical of the late stage I though the data points are scattering. The exponents γ are larger than the exponents α , indicating that the local structure changes much faster than the global

Table 2. Results on Scaling Analysis in the Late-Stage Spinodal Decomposition

specimen code	w_{block} (wt %)	temp (°C)	α^a	γ^b	$\gamma - \alpha$
B0	0	50	0.78	0.90	0.12
		60	0.77	0.92	0.15
		70	0.80	0.94	0.14
B3	3.0	50	0.66	0.81	0.15
		60	0.68	0.89	0.21
		70	0.70	0.85	0.15
B6	6.0	50	0.54	0.74	0.20
		60	0.60		
		70	0.65	0.85	0.20

^a Defined by eq 6. ^b Defined by eq 10.

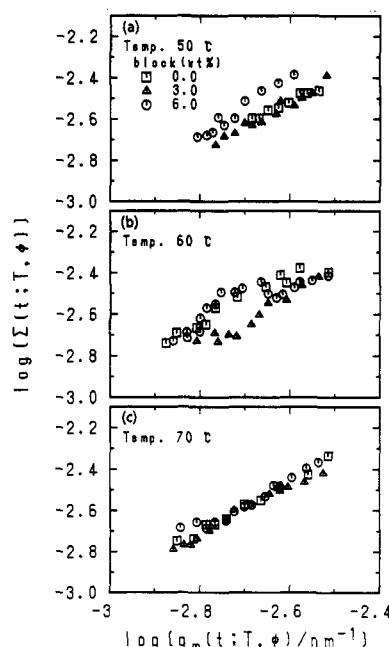


Figure 12. Plots of interfacial area density $\Sigma(t; T, \phi)$ versus peak scattering vector $q_m(t; T, \phi)$ for blends with various block copolymer compositions at (a) 50, (b) 60, and (c) 70 °C.

structure and approaches equilibrium much faster than the global structure (as shown in Figure 11 or Table 2).

Figure 12 shows a relationship between the global wavenumber $q_m(t; T, \phi)$ and the local wavenumber $\Sigma(t; T, \phi)$ for various block copolymer compositions at 50 (a), 60 (b), and 70 °C (c). It is found, within experimental accuracy, that the local wavenumbers for blends with various copolymer contents tend to be uniquely determined by the global wavenumber. This explains our earlier result shown in Figure 8. In other words, the local wavenumber decreases as the global wavenumber gets smaller in a manner which is independent of ϕ , although the dynamical scaling laws for the two quantities are different and depend on ϕ . In Figure 12, it is quite natural to see such a trend that the local wavenumbers are always greater than the global wavenumbers.

VI. Conclusion

Effects of adding a small amount of the block copolymer to polymer blends composed of the same constituent polymers as those for the block copolymer on the kinetics of later-stage SD were investigated by a time-resolved light scattering at three different temperatures in a deep quench condition. It was found that the scaled structure factors obtained for each blend at the same global size $1/q_m(t; T, \phi)$ were almost identical, independent of the amount of the block copolymer ϕ . In our previous paper,¹⁵ we reported that the scaling postulate can be extended to the local structure for the binary polymer blends without the

copolymer. However, in the case of the blends with the copolymer, the plots of $\bar{\Sigma}(\tau; T, \phi)$ versus τ for the blends with different ϕ hardly fall onto a master curve at all temperatures T studied. Thus the nonuniversality called the B-branch (or the break of the scaling postulate) was found for the local structure (as observed by $\bar{\Sigma}$) as well as for the global structure¹ (as observed by Q_m). It is also found that the interfacial area density at the same global size is almost identical, independent of ϕ , within experimental accuracy, although the block copolymer slows down the evolution of the global and local structures, affecting the dynamical scaling laws for $1/q_m(t; T, \phi)$ and $1/\Sigma(t; T, \phi)$.

Acknowledgment. The authors express their thanks to the Japan Synthetic Rubber Co. Ltd. for providing the samples.

References and Notes

- (1) Hashimoto, T.; Izumitani, T. *Macromolecules* **1993**, *26*, 3631.
- (2) Cahn, J. W.; Hilliard, J. E. *J. Chem. Phys.* **1958**, *28*, 258. Cahn, J. W. *J. Chem. Phys.* **1965**, *42*, 93. de Gennes, P. G. *J. Chem. Phys.* **1980**, *72*, 4756.
- (3) Izumitani, T.; Hashimoto, T. *J. Chem. Phys.* **1985**, *83*, 3694.
- (4) Hashimoto, T.; Itakura, M.; Shimidzu, N. *J. Chem. Phys.* **1986**, *85*, 6773.
- (5) Izumitani, T.; Takenaka, M.; Hashimoto, T. *J. Chem. Phys.* **1990**, *92*, 3213.
- (6) Langer, J. S.; Bar-on, M.; Miller, H. D. *Phys. Rev. A* **1975**, *11*, 1417. Chou, Y.; Goldburg, W. I. *Phys. Rev. A* **1979**, *20*, 2105.
- (7) Kawasaki, K. *Prog. Theor. Phys.* **1977**, *57*, 826. Kawasaki, K.; Ohta, T. *Prog. Theor. Phys.* **1978**, *59*, 362.
- (8) Siggia, E. D. *Phys. Rev. A* **1979**, *20*, 595.
- (9) Kawasaki, K. *Ann. Phys. (N.Y.)* **1984**, *154*, 319.
- (10) Binder, K.; Stauffer, D. *Phys. Rev. Lett.* **1974**, *33*, 1006. Binder, K. *Phys. Rev. B* **1977**, *15*, 4425.
- (11) Gunton, J. D.; San Miguel, M.; Sahni, P. S. In *Phase Transition and Critical Phenomena*; Domb, C., Lebowitz, J. L., Eds.; Academic: New York, 1983; Vol. 8, p 269.
- (12) Hashimoto, T.; Takenaka, M.; Izumitani, T. *Polym. Commun.* **1989**, *30*, 45.
- (13) Takenaka, M.; Izumitani, T.; Hashimoto, T. *J. Chem. Phys.* **1990**, *92*, 4566.
- (14) Hashimoto, T.; Takenaka, M.; Jinnai, H. *J. Appl. Crystallogr.* **1991**, *24*, 457.
- (15) Takenaka, M.; Hashimoto, T. *J. Chem. Phys.* **1992**, *96*, 6177.
- (16) Hashimoto, T.; Izumitani, T.; Takenaka, M. *Macromolecules* **1989**, *22*, 2293.
- (17) Hashimoto, T.; Kumaki, J.; Kawai, H. *Macromolecules* **1983**, *16*, 641.
- (18) Tanaka, H.; Hashimoto, T. *Polym. Commun.* **1988**, *29*, 212.
- (19) Hashimoto, T.; Itakura, M.; Hasegawa, H. *J. Chem. Phys.* **1986**, *85*, 6118.
- (20) Porod, G. *Kolloid Z.* **1951**, *124*, 83; **1952**, *125*, 51; **1952**, *125*, 108.
- (21) Ruland, W. *J. Appl. Crystallogr.* **1971**, *4*, 70.
- (22) Hashimoto, T.; Shibayama, M.; Kawai, H. *Macromolecules* **1980**, *13*, 1237.